ARGONNE NATIONAL LABORATORY
9700 South Cass Avenue
Argonne, Illinois 60439

Benchmarking Optimization Software with COPS*

by

Elizabeth D. Dolan† and Jorge J. Moré‡

Mathematics and Computer Science Division

Technical Report ANL/MCS-TM-246

November 2000

*This work was supported by the Mathematical, Information, and Computational Sciences Division subprogram of the Office of Advanced Scientific Computing, U.S. Department of Energy, under Contract W-31-109-Eng-38, and by the the National Science Foundation (Challenges in Computational Science) grant CDA-9726385 and (Information Technology Research) grant CCR-0082807.

†Department of Electrical and Computer Engineering, Northwestern University, and Mathematics and Computer Science Division, Argonne National Laboratory, Argonne, Illinois 60439 (dolan@mcs.anl.gov).

‡Mathematics and Computer Science Division, Argonne National Laboratory, Argonne, Illinois 60439 (more@mcs.anl.gov).

Contents

Abstract 1

Introduction 1

Testing Methods 2

1 Largest Small Polygon 3

2 Distribution of Electrons on a Sphere 5

3 Hanging Chain 7

4 Shape Optimization of a Cam 9

5 Isometrization of α-pinene 11

6 Marine Population Dynamics 13

7 Flow in a Channel 16

8 Robot Arm 18

9 Particle Steering 21

10 Goddard Rocket 23

11 Hang Glider 26

12 Catalytic Cracking of Gas Oil 29

13 Methanol to Hydrocarbons 31

14 Catalyst Mixing 33

15 Elastic-Plastic Torsion 35

16 Journal Bearing 37

17 Minimal Surface with Obstacle 39

Acknowledgments 41

References 41

Benchmarking Optimization Software with COPS

by

Elizabeth D. Dolan and Jorge J. Moré

Abstract

We describe version 2.0 of the COPS set of nonlinearly constrained optimization problems. We have added new problems, as well as streamlined and improved most of the problems. We also provide a comparison of the LANCELOT, LOQO, MINOS, and SNOPT solvers on these problems.

Introduction

The COPS [5] test set provides a modest selection of difficult nonlinearly constrained optimization problems from applications in optimal design, fluid dynamics, parameter estimation, and optimal control. In this report we describe version 2.0 of the COPS problems. The formulation and discretization of the original problems have been streamlined and improved. We have also added new problems.

The presentation of COPS follows the original report, but the description of the problems has been streamlined. For each problem we discuss the formulation of the problem and the structural data in Table 0.1 on the formulation. The aim of presenting this data is to provide an approximate idea of the size and sparsity of the problem.

Table 0.1: Description of test problems

Variables
Constraints
Bounds
Linear equality constraints
Linear inequality constraints
Nonlinear equality constraints
Nonlinear inequality constraints
Nonzeros in $\nabla^2 f(x)$
Nonzeros in $c'(x)$

We also include the results of computational experiments with the LANCELOT, LOQO, MINOS, and SNOPT solvers. These computational experiments differ from the original [5] results in that we have deleted problems that were considered to be too easy. Moreover, in the current version of the computational experiments, each problem is tested with four variations.

An important difference between this report and the original [5] report is that the tables that present the computational experiments are generated automatically from the testing script. This is explained in more detail in the following section, Testing Methods.

Testing Methods

We have performed our trials on sixty-eight variants of seventeen different applications, which constitute version 2.0 of the COPS set. The implementations are written in the AMPL modeling language for use with the AMPL (version 20000906) interfaces to nonlinearly constrained optimization solvers of interest to us. The solvers include LANCELOT (AMPL driver 19990513), LOQO 5.03 (20000528), MINOS 5.5 (19981015), and SNOPT 5.3-4 (19981124).

We have devised a script for running a problem on each solver successively, so as to minimize the effect of fluctuation in the machine load. The script tracks the wall-clock time from the start of the solve, killing any process that runs for more than 3,600 seconds, which we declare unsuccessful. We cycle through all problem variants, recording the wall-clock time as well as the combination of AMPL system time (to interpret the model and compute varying amounts of derivative information required by each solver) and solver time. We consider the times returned by AMPL definitive, but we initially record the wall-clock times to check for discrepancies in the solvers' methods of calculating execution time. We include no problem results for which the AMPL time and the wall-clock time differ by more than ten percent. To further ensure consistency, we have verified that the AMPL time results we present could be reproduced to within ten percent accuracy. All computations were done on a SparcULTRA2 running Solaris 7.

Once all the runs have completed, a parser searches the output files for key text patterns indicating whether the solver completed successfully. The script then gathers the data we need into tables and other files for later calculations.

The AMPL interfaces to these solvers provide numerous options. We set options for each solver and execute our final complete runs with the same options for all problems. The options involve setting the output level so that we can gather the data we want, increasing the iteration limits as much as allowed, and increasing the super-basics limits for MINOS and SNOPT to 5000. None of the failures we record in the final trials include any solver error messages about having violated these limits.

We realize that testing optimization software is a notoriously difficult problem and that there may be objections to the testing presented in this report. For example, performance of a particular solver may improve significantly if non-default options are given. Another objection is that we only use one starting point per problem and that the performance of a solver may be sensitive to the choice of starting point. We also have used the default stopping criteria of the solvers. This choice may bias results but should not affect comparisons that rely on large time differences. In spite of these objections, we feel that it is essential that we provide some indication of the performance of optimization solvers on interesting problems. This report is an effort in this direction.

1 Largest Small Polygon

Find the polygon of maximal area, among polygons with n_v sides and diameter $d \leq 1$.

Formulation

This is a classic problem (see, for example, Graham [16]). If (r_i, θ_i) are the coordinates of the vertices of the polygon, then we must minimize

$$f(r,\theta) = -\tfrac{1}{2} \sum_{i=1}^{n_v-1} r_{i+1} r_i \sin(\theta_{i+1} - \theta_i)$$

subject to the constraints

$$\begin{aligned} r_i^2 + r_j^2 - 2 r_i r_j \cos(\theta_i - \theta_j) \leq 1, \qquad & 1 \leq i \leq n_v, \quad i < j \leq n_v, \\ \theta_i \leq \theta_{i+1}, \qquad & 1 \leq i < n_v, \\ \theta_i \in [0,\pi],\ r_i \geq 0, \qquad & 1 \leq i \leq n_v. \end{aligned}$$

Our implementation follows [14] and fixes the last vertex by setting $r_{n_v} = 0$ and $\theta_{n_v} = \pi$. By fixing a vertex at the origin, we can add the bounds $r_i \leq 1$.

The optimal solution is not usually a regular hexagon, as was shown by Graham [16]. Another interesting feature of this problem is the presence of order n_v^2 nonlinear nonconvex inequality constraints. We also note that as $n_v \to \infty$, we expect the maximal area to converge to the area of a unit-diameter circle, $\pi/4 \approx 0.7854$. This problem has many local minima. For example, for $n_v = 4$ a square with sides of length $1/\sqrt{2}$ and an equilateral triangle with another vertex added at distance 1 away from a fixed vertex are both global solutions with optimal value $f = \frac{1}{2}$. Indeed, the number of local minima is at least $O(n_v!)$. Thus, general solvers are usually expected to find only local solutions. Data for this problem appears in Table 1.1.

Table 1.1: Largest-small polygon problem data

Variables	$2n_v$
Constraints	$(\frac{1}{2}n_v + 1)(n_v - 1)$
Bounds	$2n_v$
Linear equality constraints	0
Linear inequality constraints	$n_v - 1$
Nonlinear equality constraints	0
Nonlinear inequality constraints	$\frac{1}{2}n_v(n_v - 1)$
Nonzeros in $\nabla^2 f(x)$	$6n_v$
Nonzeros in $c'(x)$	$2n_v(n_v - 1)$

Performance

Results for the AMPL implementation are summarized in Table 1.2. A polygon with almost equal sides is the starting point. Global solutions for several n_v are shown in Figure 1.1.

Table 1.2: Performance on largest small polygon problem

Solver	$n_v = 25$	$n_v = 50$	$n_v = 75$	$n_v = 100$
LANCELOT	12.83 s	398.12 s	1148.2 s	‡
f	7.79715e-01	7.83677e-01	7.84747e-01	‡
c violation	8.89750e-06	1.40500e-06	2.81600e-06	‡
iterations	61	192	176	‡
LOQO	3.49 s	30.16 s	268.9 s	‡
f	7.64714e-01	7.77520e-01	7.77554e-01	‡
c violation	1.2e-09	4.0e-09	1.4e-09	‡
iterations	110	203	566	‡
MINOS	2.11 s	28.45 s	98.54 s	344.81 s
f	7.64383e-01	6.57163e-01	7.60729e-01	7.72803e-01
c violation	1.2e-13	2.2e-16	2.7e-13	1.3e-10
iterations	280	1552	2166	5184
SNOPT	1.14 s	12.69 s	91.07 s	256.6 s
f	7.79740e-01	7.84016e-01	7.84769e-01	7.85040e-01
c violation	2.9e-10	9.1e-10	1.1e-09	1.5e-07
iterations	91	244	499	752

† Errors or warnings. ‡ Timed out.

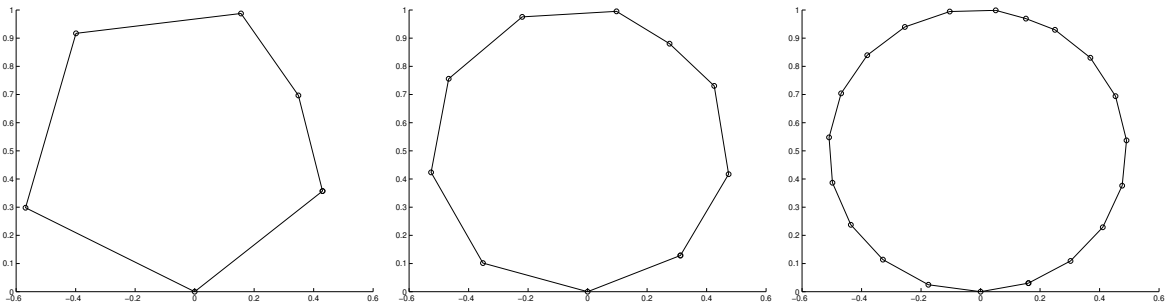

Figure 1.1: Polygons of maximal area with $n_v = 6, 10, 20$ (left, center, right)

2 Distribution of Electrons on a Sphere

Given n_p electrons, find the equilibrium state distribution (of minimal Coulomb potential) of the electrons positioned on a conducting sphere.

Formulation

This problem, known as the Thomson problem of finding the lowest energy configuration of n_p point charges on a conducting sphere, originated with Thomson's plum pudding model of the atomic nucleus. This problem is representative of an important class of problems in physics and chemistry that determine a structure with respect to atomic positions.

The potential energy for n_p points (x_i, y_i, z_i) is defined by

$$f(x,y,z) = \sum_{i=1}^{n_p-1} \sum_{j=i+1}^{n_p} \left((x_i - x_j)^2 + (y_i - y_j)^2 + (z_i - z_j)^2\right)^{-\frac{1}{2}},$$

and the constraints on the n_p points are

$$x_i^2 + y_i^2 + z_i^2 = 1, \qquad i = 1, \ldots, n_p.$$

Data for this problem appears in Table 2.1.

This problem has many local minima at which the objective value is relatively close to the objective value at the global minimum. Experimental and theoretical results [18, 20] show that

$$\min\left\{f(v_1, \ldots, v_{n_p}) : \|v_i\| = 1,\ 1 \le i \le n_p\right\} \ge \tfrac{1}{2} n_p^2 (1 - \varepsilon), \qquad 0 \le \varepsilon \le \left(\frac{1}{n_p}\right)^{1/2}.$$

Also, the number of local minima grows exponentially with n_p. Thus, determining the global minimum is computationally difficult, and solvers are usually expected to find only a local minimum.

Table 2.1: Electrons on a sphere problem data

Variables	$3n_p$
Constraints	n_p
Bounds	0
Linear equality constraints	0
Linear inequality constraints	0
Nonlinear equality constraints	n_p
Nonlinear inequality constraints	0
Nonzeros in $\nabla^2 f(x)$	$9n_p^2$
Nonzeros in $c'(x)$	$3n_p$

Performance

Results for the AMPL implementation are summarized in Table 2.2. The starting point is a quasi-uniform distribution of the points on a unit sphere. The best solution for $n_p = 100$ is shown in Figure 2.1.

Table 2.2: Performance on electrons on a sphere problem

Solver	$n_p = 25$	$n_p = 50$	$n_p = 100$	$n_p = 200$
LANCELOT	3.98 s	8.08 s	53.36 s	371.6 s
f	2.43812e+02	1.05518e+03	4.44841e+03	1.84389e+04
c violation	2.34380e-06	2.58920e-08	2.32410e-07	1.94010e-06
iterations	50	46	67	127
LOQO	0.84 s	7.94 s	179.06 s	2437.78 s
f	2.43812e+02	1.05518e+03	4.44835e+03	1.84389e+04
c violation	2.8e-09	4.9e-09	3.0e-09	1.9e-09
iterations	27	46	130	264
MINOS	6.22 s	36.85 s	‡	794.08 s
f	2.43812e+02	1.05518e+03	‡	1.25964e+04†
c violation	7.7e-08	1.2e-12	‡	6.6e+09†
iterations	1273	1951	‡	1480
SNOPT	9.65 s	10.68 s	73.66 s	1600.48 s
f	2.43812e+02	1.05518e+03	4.44841e+03	1.84390e+04
c violation	2.2e-09	1.8e-10	5.2e-10	9.0e-10
iterations	245	253	448	1171

† Errors or warnings. ‡ Timed out.

MINOS cannot solve the problem for $n_p > 50$. For $n_p = 200$ it gives the error message *unbounded (or badly scaled) problem.*

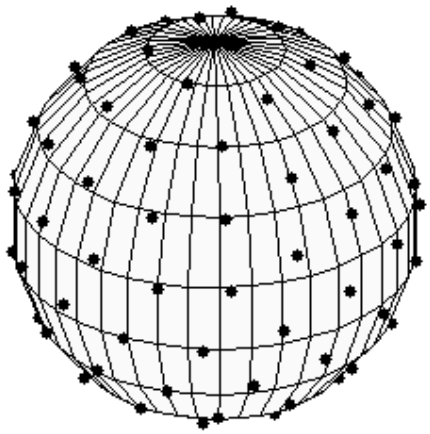

Figure 2.1: Optimal distribution of electrons on a sphere, $n_p = 100$

3 Hanging Chain

Find the chain (of uniform density) of length L suspended between two points with minimal potential energy.

Implementation

This classical problem (see Cesari [11, pages 126–127]) was suggested by Hans Mittelmann. In this problem we need to determine a function $x(t)$, the shape of the chain, that minimizes the potential energy

$$\int_0^1 x\sqrt{1+x'^2}\,dt$$

subject to the constraint on the length of the chain,

$$\int_0^1 \sqrt{1+x'^2}\,dt = L,$$

and the end conditions $x(0) = a$ and $x(1) = b$. We reformulate this problem as a control problem in terms of the function $u = x'$. The optimal control version of the problem is

$$\int_0^1 x\sqrt{1+u^2}\,dt$$

subject to a differential equation and a constraint on the length of the chain,

$$x' = u, \qquad \int_0^1 \sqrt{1+u^2}\,dt = L.$$

We discretize the integrals and the differential equation with the trapezoidal rule on a uniform mesh with n_h intervals. Data for this problem appears in Table 3.1.

Table 3.1: Hanging chain problem data

Variables	$2n_h$
Constraints	$n_h + 1$
Bounds	0
Linear equality constraints	n_h
Linear inequality constraints	0
Nonlinear equality constraints	1
Nonlinear inequality constraints	0
Nonzeros in $\nabla^2 f(x)$	$3n_h$
Nonzeros in $c'(x)$	$5n_h$

Performance

Results for the AMPL implementation are summarized in Table 3.2 with $a = 1$, $b = 3$, and $L = 4$. The starting point is the quadratic

$$x(t) = (2|b-a|)\,t(t-2t_m) + a,$$

where $t_m = 0.25$ if $b > a$ and $t_m = 0.75$ otherwise, evaluated at the mesh points. This choice is convex and satisfies the boundary data. The control function u is set to x'. The optimal chain is shown in Figure 3.1.

Table 3.2: Performance on hanging chain problem

Solver	$n_h = 50$	$n_h = 100$	$n_h = 200$	$n_h = 400$
LANCELOT	13.91 s	42.79 s	268.7 s	577.24 s
f	5.07230e+00	5.07005e+00	5.06903e+00	5.06788e+00
c violation	3.31310e-06	9.61060e-06	2.01200e-06	6.25860e-06
iterations	772	1169	3042	3203
LOQO	17.24 s	6.69 s	174.58 s	1028.35 s
f	5.07226e+00	5.06978e+00	5.06891e+00	5.06862e+00
c violation	3.3e-08	7.3e-10	5.7e-10	2.4e-09
iterations	773	206	758	777
MINOS	1.22 s	5.52 s	14.75 s	73.9 s
f	5.07226e+00	5.06978e+00	5.06891e+00	5.06862e+00
c violation	6.1e-08	4.0e-07	2.5e-06	3.3e-06
iterations	428	765	1104	2312
SNOPT	5.72 s	32.76 s	52.8 s	‡
f	5.07226e+00	5.06978e+00	5.06891e+00	‡
c violation	5.9e-09	5.2e-09	1.6e-06	‡
iterations	265	451	487	‡

† Errors or warnings. ‡ Timed out.

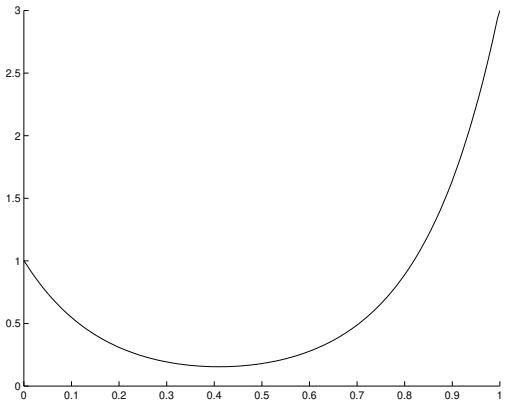

Figure 3.1: Hanging chain of length $L = 4$

4 Shape Optimization of a Cam

Maximize the area of the valve opening for one rotation of a convex cam with constraints on the curvature and on the radius of the cam.

Formulation

The formulation of this problem is due to Anitescu and Serban [1]. We assume that the shape of the cam is circular over an angle of $\frac{6}{5}\pi$ of its circumference, with radius $r_{\min}$. The design variables r_i, $i = 1, \ldots, n$, represent the radius of the cam at equally spaced angles distributed over an angle of $\frac{2}{5}\pi$. We maximize the area of the valve opening by maximizing

$$f(r) = \pi r_v^2 \left(\frac{1}{n} \sum_{i=1}^{n} r_i \right)$$

subject to the constraints on r. The design parameter r_v is related to the geometry of the valve. We also require that $r_{\min} \leq r_i \leq r_{\max}$. The requirement that the cam be convex is expressed by requiring that

$$\text{area}(r_{i-1}, r_{i+1}) \leq \text{area}(r_{i-1}, r_i) + \text{area}(r_i, r_{i+1}),$$

where $\text{area}(r_i, r_j)$ is the area of the triangle defined by the origin and the points r_i and r_j on the cam surface. This convexity constraint can also be expressed as

$$2r_{i-1}r_{i+1}\cos(\theta) \leq r_i(r_{i-1} + r_{i+1}), \qquad i = 0, \ldots, n+1,$$

where $r_{-1} = r_0 = r_{\min}$, $r_{n+1} = r_{\max}$, $r_{n+2} = r_n$ and $\theta = 2\pi/5(n+1)$. The curvature requirement is expressed by

$$-\alpha \leq \left(\frac{r_{i+1} - r_i}{\theta} \right) \leq \alpha, \qquad i = 0, \ldots, n.$$

This is a departure from [1], where the curvature constraint was expressed in terms of $(r_{i+1} - r_i)^2$. Data for this problem appears in Table 4.1.

Table 4.1: Optimal design of a cam problem data

Variables	n
Constraints	$2n + 2$
Bounds	n
Linear equality constraints	0
Linear inequality constraints	n + 1
Nonlinear equality constraints	0
Nonlinear inequality constraints	$n + 1$
Nonzeros in $\nabla^2 f(x)$	0
Nonzeros in $c'(x)$	$5n$

We follow [1] and use $r_{\min} = 1.0$ and $r_{\max} = 2.0$ for the bounds on r, $r_v = 1.0$ in the area of the valve, and $\alpha = 1.5$ in the curvature constraint. Since the optimal cam shape is symmetric, we consider only half of the design angle. The problem was originally [1] formulated for the full angle of $\frac{4}{5}\pi$.

Performance

Results for the AMPL implementation are summarized in Table 4.2. We use a starting guess of $r_i \equiv (r_{\min} + r_{\max})/2$. The cam shape for $\alpha = 1.5$ appears in Figure 4.1. We note that the number of active constraints increases with α up to a threshold of $\alpha_1 \approx 3.0$, after which increasing α does not change the optimal solution.

Table 4.2: Performance on optimal cam shape problem

Solver	$n = 100$	$n = 200$	$n = 400$	$n = 800$
LANCELOT	42.74 s	194.89 s	1025.23 s	1887.03 s
f	4.30178e+00†	4.35538e+00†	4.45009e+00†	4.85693e+00
c violation	4.50980e-06†	5.14160e-06†	3.22630e-06†	4.50740e-06
iterations	316	491	767	773
LOQO	0.68 s	1.51 s	4.65 s	12.47 s
f	4.28414e+00	4.27850e+00	4.27568e+00	4.27427e+00
c violation	2.1e-12	1.9e-11	2.3e-13	1.7e-12
iterations	63	73	113	117
MINOS	0.87 s	1.32 s	4.59 s	21.72 s
f	4.28414e+00	4.27850e+00	4.27567e+00†	4.27426e+00
c violation	4.4e-16	1.4e-14	9.3e-14†	3.0e-13
iterations	474	428	765	2416
SNOPT	0.6 s	1.79 s	6.48 s	25.17 s
f	4.28414e+00	4.27340e+00	4.27022e+00	4.23739e+00
c violation	1.3e-15	1.8e-07	2.3e-06	6.2e-07
iterations	312	584	1121	2235

† Errors or warnings. ‡ Timed out.

LANCELOT stops prematurely with the message *step got too small* for $n = 100$, 200, 400; and its solution for $n = 800$, while showing the best value, violates the problem constraints to an extent obvious in a graph of the solution. MINOS quits for $n = 400$ because *the current point cannot be improved.*

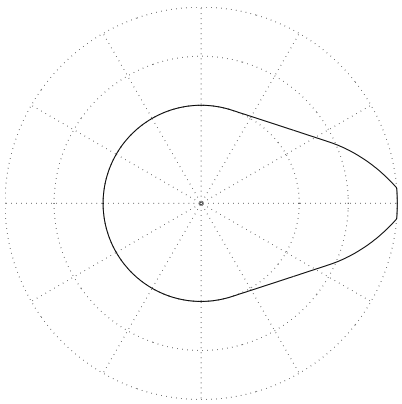

Figure 4.1: Cam shape for $\alpha = 1.5$.

5 Isometrization of α-pinene

Determine the reaction coefficients in the thermal isometrization of α-pinene. The linear kinetic model [6] is

$$\begin{aligned} y_1' &= -(\theta_1+\theta_2)y_1 \\ y_2' &= \theta_1 y_1 \\ y_3' &= \theta_2 y_1 - (\theta_3+\theta_4)y_3 + \theta_5 y_5 \\ y_4' &= \theta_3 y_3 \\ y_5' &= \theta_4 y_3 - \theta_5 y_5, \end{aligned} \tag{5.1}$$

where $\theta_i \geq 0$ are the reaction coefficients. Initial conditions for (5.1) are known. The problem is to minimize

$$\sum_{j=1}^{8} \|y(\tau_j;\theta) - z_j\|^2, \tag{5.2}$$

where z_j are concentration measurements for y at time points $\tau_1, \ldots, \tau_8$.

Formulation

Our formulation of the α-pinene problem as an optimization problem follows [21, 3]. We use a k-stage collocation method, a uniform partition with n_h subintervals of $[0, \tau_8]$, and the standard [2, pages 247–249] basis representation,

$$v_i + \sum_{j=1}^{k} \frac{(t-t_i)^j}{j!\, h^{j-1}} w_{ij}, \qquad t \in [t_i, t_{i+1}],$$

for the components of the solution y of (5.1). The constraints in the optimization problem are the initial conditions in (5.1), the continuity conditions, and the collocation equations. The continuity equations at each interior grid point are a set of $5(n_h - 1)$ linear equations. The collocation equations are a set of $5kn_h$ nonlinear equations obtained by requiring that the collocation approximation satisfy (5.1) at the collocation points. Data for this problem appears in Table 5.1.

Table 5.1: Isometrization of α-pinene data

Variables	$5(k+1)n_h + 5$
Constraints	$5(k+1)n_h$
Bounds	5
Linear equality constraints	$5n_h$
Linear inequality constraints	0
Nonlinear equality constraints	$5kn_h$
Nonlinear inequality constraints	0
Nonzeros in $\nabla^2 f(x)$	$40(k+1)^2$
Nonzeros in $c'(x)$	$10k(k+1)n_h$

Performance

We provide results for the AMPL formulation with $k = 3$ in Table 5.2. The initial values for the θ parameters are $\theta_i = 0.0$. The initial basis parameters are chosen so that the collocation approximation is piecewise constant and interpolates the data. The solution and data are shown in Figure 5.1.

Table 5.2: Performance on isometrization problem

Solver	$n_h = 25$	$n_h = 50$	$n_h = 100$	$n_h = 200$
LANCELOT	1426.01 s	2720.49 s	‡	‡
f	1.96766e+01†	1.93937e+01†	‡	‡
c violation	1.87900e-06†	6.09920e-06†	‡	‡
iterations	305	179	‡	‡
LOQO	28.85 s	6.15 s	6.77 s	16.87 s
f	1.98715e+01	1.98721e+01	1.98721e+01	1.98721e+01
c violation	1.3e-11	2.2e-13	7.6e-13	8.4e-13
iterations	389	32	23	21
MINOS	1.98 s	6.74 s	21.66 s	194.84 s
f	1.98715e+01	1.98721e+01	1.98721e+01	0.00000e+00†
c violation	4.2e-13	4.4e-13	2.3e-12	1.7e+04†
iterations	378	736	1354	3279
SNOPT	3.74 s	13.1 s	48.91 s	235.44 s
f	1.98715e+01	1.98721e+01†	1.98721e+01	1.98721e+01†
c violation	3.9e-13	4.2e-13†	6.7e-13	5.1e-13†
iterations	570	1072	2060	4087

† Errors or warnings. ‡ Timed out.

LANCELOT stops with the message *step got too small*, near the solution for $n_h \leq 50$. MINOS fails completely on $n_h = 200$ with *unbounded (or badly scaled) problem*, while SNOPT manages a *[p]rimal feasible solution*, which *could not satisfy dual feasibility* for both $n_h = 50,\ 200$.

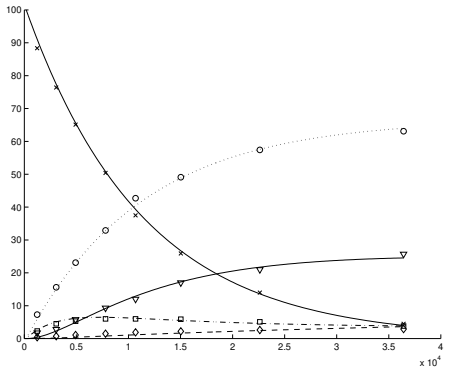

Figure 5.1: Solution and data for the α-pinene problem

6 Marine Population Dynamics

Given estimates of the abundance of the population of a marine species at each stage (for example, nauplius, juvenile, adult) as a function of time, determine stage specific growth and mortality rates. The model for the population dynamics of the n_s-stage population is

$$y_j' = g_{j-1}y_{j-1} - (m_j + g_j)y_j, \qquad 1 \le j \le n_s, \tag{6.1}$$

where m_i and g_i are the unknown mortality and growth rates at stage i with $g_0 = g_{n_s} = 0$. This model assumes that the species eventually dies or grows into the next stage, with the implicit assumption that the species cannot skip a stage. Initial conditions for the differential equations are unknown, since the stage abundance measurements at the initial time might also be contaminated with experimental error. We minimize the error between computed and observed data,

$$\sum_{j=1}^{n_m} \|y(\tau_j; m, g) - z_j\|^2,$$

where z_j are the stage abundance measurements. This problem is based on the work of Rothschild, Sharov, Kearsley, and Bondarenko [19].

Formulation

Our formulation of the marine population dynamics uses a k-stage collocation method, a uniform partition with n_h subintervals of $[0, \tau_{n_m}]$, and the standard [2, pages 247–249] basis representation,

$$v_i + \sum_{j=1}^{k} \frac{(t - t_i)^j}{j!\, h^{j-1}} w_{ij}, \qquad t \in [t_i, t_{i+1}],$$

for the components of the solution y of (6.1). The constraints in the optimization problem are the continuity conditions and the collocation equations. The continuity equations are a set of $n_s(n_h - 1)$ linear equations. The collocation equations are a set of $k\, n_s\, n_h$ nonlinear equations obtained by requiring that the collocation approximation satisfy (6.1) at the collocation points $\xi_{ij} = t_i + h\rho_j$ for $i = 1, \ldots, n_h$ and $j = 1, \ldots, k$.

Table 6.1: Marine population dynamics problem data

Variables	$(k+1)n_s n_h + 2n_s - 1$
Constraints	$(k+1)n_s n_h - n_s$
Bounds	$2n_s - 1$
Linear equality constraints	$n_s(n_h - 1)$
Linear inequality constraints	0
Nonlinear equality constraints	$kn_s n_h$
Nonlinear inequality constraints	0
Nonzeros in $\nabla^2 f(x)$	$(k+1)^2 n_s n_m$
Nonzeros in $c'(x)$	$(2k+1)(k+2)n_s n_h$

The parameters in the problem are the $n_s n_h$ initial conditions, the n_s mortality rates, the $n_s - 1$ growth rates, and the $(k+1)n_s n_h$ basis parameters in the representation of the collocation approximation. Data for this problem appears in Table 6.1.

We do not impose any initial conditions on the differential equations, since initial measurements are usually contaminated with experimental error. Introducing these extra degrees of freedom into the problem formulation should allow solvers to find a better fit to the data. A significant difference between this problem and other parameter estimation problems is that the population dynamics data usually contains large observation errors.

Performance

We provide results for the AMPL formulation with $k = 2$ in Table 6.2. We use a simulated dataset with $n_s = 8$ stages. The initial basis parameters are chosen so that the collocation approximation is piecewise constant and interpolates the data.

Table 6.2: Performance on marine population dynamics problem

Solver	$n_h = 25$	$n_h = 50$	$n_h = 100$	$n_h = 200$
LANCELOT	623.75 s	1084.33 s	3170.26 s	‡
f	1.97522e+07†	1.97465e+07†	1.97465e+07†	‡
c violation	1.80930e-06†	3.27200e-06†	6.49480e-06†	‡
iterations	245	281	243	‡
LOQO	2.07 s	4.64 s	12.53 s	38.4 s
f	1.97522e+07	1.97465e+07	1.97465e+07	1.97465e+07
c violation	5.3e-10	7.0e-10	5.8e-11	2.8e-10
iterations	25	25	27	27
MINOS	6.58 s	15.75 s	167.83 s	245.1 s
f	1.97522e+07	1.97465e+07	2.17862e+07	0.00000e+00†
c violation	4.5e-12	5.3e-11	4.2e-08	3.4e+05†
iterations	531	867	2761	2260
SNOPT	85.37 s	184.4 s	477.59 s	1502.26 s
f	1.97522e+07	1.97465e+07	1.97465e+07	1.97465e+07
c violation	4.5e-12	1.1e-11	7.3e-12	2.0e-11
iterations	1235	1800	3031	5563

† Errors or warnings. ‡ Timed out.

LANCELOT returns the message *step got too small* for the values of n_h for which it terminates within $3,600$ wall-clock seconds. The intermediate solution returned by LANCELOT upon termination is in close agreement with the optimal solutions returned by the other solvers. MINOS makes no progress with $n_h = 200$, returning with the error *unbounded (or badly scaled) problem.*

The graph on the left of Figure 6.1 shows the populations for stages $1, 2, 5,$ and 6, while the graph on the right shows the populations for stages $3, 4, 7,$ and 8. In both cases, the fit between the model and the data is not always tight.

For this problem we are using a relatively small number of collocation points ($k = 2$), since in this case the number of parameters grows quickly with the number of stages. The quality of the solution does not seem to be affected, at least as measured by the population

curves and the mortality and growth parameters.

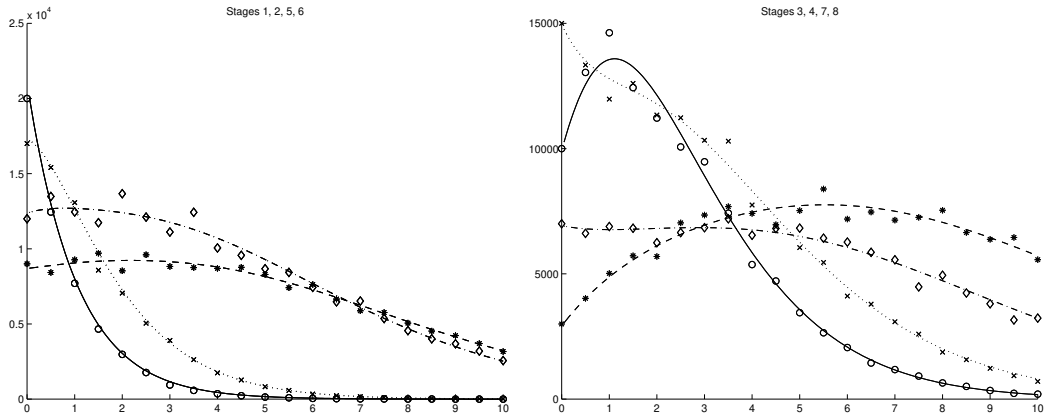

Figure 6.1: Marine populations for stages $1, 2, 5, 6$ (left) and $3, 4, 7, 8$ (right)

Figure 6.2 plots the mortality and growth parameters for the eight stages. Mortality parameters are marked $*$, while growth parameters are marked $\circ$. The mortality parameters for stages 5 and 6 are not zero, but they are on the order of 10^{-3} and 10^{-9}, respectively.

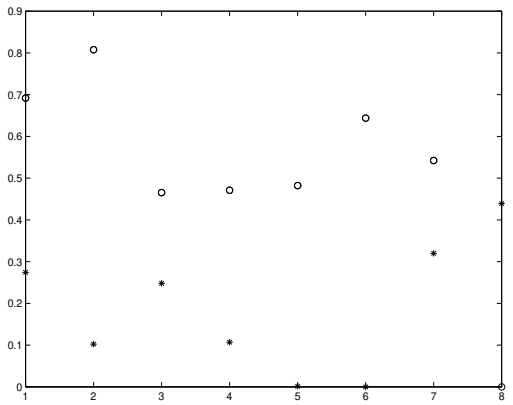

Figure 6.2: Mortality $(*)$ and growth $(\circ)$ parameters for the marine populations stages

7 Flow in a Channel

Analyze the flow of a fluid during injection into a long vertical channel, assuming that the flow is modeled by the boundary value problem

$$\begin{aligned} &u'''' = R\,(u'u'' - uu'''), \qquad 0 \le t \le 1, \\ &u(0) = 0, \quad u(1) = 1, \quad u'(0) = u'(1) = 0, \end{aligned} \tag{7.1}$$

where u is the potential function, u' is the tangential velocity of the fluid, and R is the Reynolds number.

Formulation

We use a k-stage collocation method to formulate this problem as an optimization problem with a constant merit function and equality constraints representing the solution of (7.1). We use a uniform partition with n_h subintervals of $[0, 1]$, and the standard [2, pages 247–249] basis representation,

$$u(t) = \sum_{j=1}^{m} \frac{(t - t_i)^{j-1}}{(j-1)!} v_{ij} + \sum_{j=1}^{k} \frac{(t - t_i)^{j+m-1}}{(j+m-1)!\, h^{j-1}} w_{ij}, \qquad t \in [t_i, t_{i+1}],$$

for u. Note that $u \in C^{m-1}[0, 1]$, where $m = 4$ is the order of the differential equation.

The constraints in the optimization problem are the initial conditions in (7.1), the continuity conditions, and the collocation equations. There are $m = 4$ initial conditions. The continuity equations are a set of $m(n_h - 1)$ linear equations. The collocation equations are a set of $k\,n_h$ nonlinear equations obtained by requiring that u satisfy (7.1) at the collocation points $\xi_{ij} = t_i + h\rho_j$ for $i = 1, \ldots, n_h$ and $j = 1, \ldots, k$. The collocation points ρ_j are the roots of the kth degree Legendre polynomial. The parameters in the optimization problem are the $(m+k)n_h$ parameters v_{ij} and w_{ij} in the representation of u. Data for this problem appears in Table 7.1.

Table 7.1: Flow in a channel problem data

Variables	$(k+4)n_h$
Constraints	$(k+4)n_h$
Bounds	0
Linear equality constraints	$4n_h$
Linear inequality constraints	0
Nonlinear equality constraints	kn_h
Nonlinear inequality constraints	0
Nonzeros in $\nabla^2 f(x)$	0
Nonzeros in $c'(x)$	$k(k+8)n_h$

Performance

Results for the AMPL implementation with $k = 4$ and $R = 10$ are summarized in Table 7.2. The starting point is the function $t^2(3 - 2t)$ evaluated at the mesh points. Solutions for

several R are shown in Figure 7.1. This problem is easy to solve for small Reynolds numbers but becomes increasingly difficult to solve as R increases.

Table 7.2: Performance on flow in channel problem

Solver	$n_h = 50$	$n_h = 100$	$n_h = 200$	$n_h = 400$
LANCELOT	‡	‡	‡	‡
f	‡	‡	‡	‡
c violation	‡	‡	‡	‡
iterations	‡	‡	‡	‡
LOQO	1.55 s	2.59 s	7.03 s	22.54 s
f	1.00000e+00	1.00000e+00	1.00000e+00	1.00000e+00
c violation	5.1e-12	1.1e-11	2.9e-11	1.9e-11
iterations	32	25	29	35
MINOS	1.09 s	3.25 s	11.15 s	32.65 s
f	1.00000e+00	1.00000e+00	1.00000e+00	1.00000e+00
c violation	3.8e-13	2.4e-13	2.0e-13	3.8e-07
iterations	151	301	601	999
SNOPT	2.14 s	7.47 s	27.91 s	98.5 s
f	1.00000e+00	1.00000e+00	1.00000e+00	1.00000e+00
c violation	6.1e-05	4.6e-05	4.1e-05	3.9e-05
iterations	398	798	1598	2994

† Errors or warnings. ‡ Timed out.

LANCELOT is unable to solve even simple versions of the problem, advancing very slowly toward the solution (as judged from the value of the merit function).

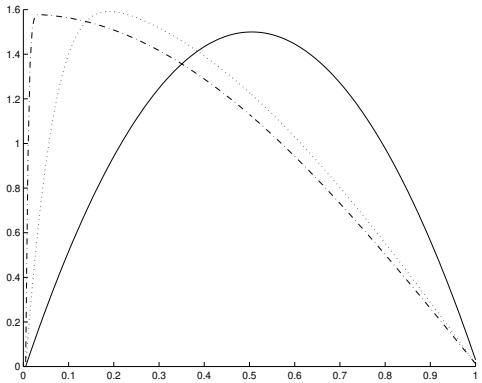

Figure 7.1: Tangential velocity u' for Reynolds numbers $R = 0, 10^2, 10^4$

8 Robot Arm

Minimize the time taken for a robot arm to travel between two points.

Formulation

This problem originated in the thesis of Monika Mössner-Beigel (Heidelberg University). In her formulation the arm of the robot is a rigid bar of length L that protrudes a distance ρ from the origin to the gripping end and sticks out a distance $L - \rho$ in the opposite direction. If the pivot point of the arm is the origin of a spherical coordinate system, then the problem can be phrased in terms of the length ρ of the arm from the pivot, the horizontal and vertical angles (θ, ϕ) from the horizontal plane, the controls $(u_\rho, u_\theta, u_\phi)$, and the final time t_f. Bounds on the length and angles are

$$\rho(t) \in [0, L], \qquad |\theta(t)| \leq \pi, \qquad 0 \leq \phi(t) \leq \pi,$$

and for the controls,

$$|u_\rho| \leq 1, \qquad |u_\theta| \leq 1, \qquad |u_\phi| \leq 1.$$

The equations of motion for the robot arm are

$$L\rho'' = u_\rho, \qquad I_\theta \theta'' = u_\theta, \qquad I_\phi \phi'' = u_\phi, \tag{8.1}$$

where I is the moment of inertia, defined by

$$I_\theta = \frac{((L-\rho)^3 + \rho^3)}{3} \sin(\phi)^2, \qquad I_\phi = \frac{((L-\rho)^3 + \rho^3)}{3}.$$

The boundary conditions are

$$\rho(0) = \rho(t_f) = 4.5, \qquad \theta(0) = 0,\ \theta(t_f) = \frac{2\pi}{3}, \qquad \phi(0) = \phi(t_f) = \frac{\pi}{4},$$

$$\rho'(0) = \theta'(0) = \phi'(0) = \rho'(t_f) = \theta'(t_f) = \phi'(t_f) = 0.$$

This model ignores the fact that the spherical coordinate reference frame is a noninertial frame and should have terms for coriolis and centrifugal forces.

Implementation

In the implementation of Vanderbei [22] the controls u are eliminated by substitution, and thus the equality constraints in (8.1) become the inequalities

$$|L\rho''| \leq 1, \qquad |I_\theta \theta''| \leq 1, \qquad |I_\phi \phi''| \leq 1.$$

In this implementation (8.1) is expressed in terms of a first-order system with the additional variables ρ', θ', and ϕ'. Discretization is done with a uniform time step and the trapezoidal rule over n_h intervals. Data for this problem is shown in Table 8.1.

Table 8.1: Robot arm problem data

Variables	$9(n_h+1)+1$
Constraints	$6n_h$
Bounds	$6(n_h+1)$
Linear equality constraints	0
Linear inequality constraints	0
Nonlinear equality constraints	$6n_h$
Nonlinear inequality constraints	0
Nonzeros in $\nabla^2 f(x)$	0
Nonzeros in $c'(x)$	$36n_h$

Performance

Results for the AMPL implementation appear in Table 8.2. All solvers were given the same initial values. The initial values for ρ and ϕ were set to the functions $\rho \equiv 4.5$ and $\phi \equiv \pi/4$ evaluated at the grid points. Similarly, initial values for θ were set to the discrete version of the parabola

$$\theta(t) = \frac{2\pi}{3}\left(\frac{t}{t_f}\right)^2,$$

which matches three of the boundary conditions. The initial values for all the controls were set to zero, and $t_f = 1$ initially.

Table 8.2: Performance on robotic arm problem

Solver	$n_h = 50$	$n_h = 100$	$n_h = 200$	$n_h = 400$
LANCELOT	0.47 s	0.53 s	1.2 s	2.59 s
f	0.00000e+00†	-2.77555e-17†	-2.77555e-17†	-2.77555e-17†
c violation	4.18880e-02†	2.09440e-02†	1.04720e-02†	5.23600e-03†
iterations	5	3	3	3
LOQO	1.03 s	2.77 s	‡	‡
f	9.14687e+00	9.14267e+00	‡	‡
c violation	2.4e-10	4.7e-11	‡	‡
iterations	24	30	‡	‡
MINOS	2.82 s	9.89 s	37.96 s	161.18 s
f	9.14687e+00	9.14267e+00	9.14138e+00	9.14108e+00
c violation	2.0e-13	1.0e-10	2.7e-12	5.7e-13
iterations	234	427	766	1368
SNOPT	10.22 s	30.7 s	317.52 s	2671.63 s
f	9.14687e+00	1.92751e+01†	9.14142e+00	9.14101e+00
c violation	1.9e-10	3.4e-04†	1.4e-10	2.1e-10
iterations	891	1987	2597	5255

† Errors or warnings. ‡ Timed out.

LANCELOT reports that it *could not find a feasible solution* for any of the versions we try for this implementation. For $n_h = 100$, SNOPT encounters difficulties, which it describes as an *error evaluating nonlinear expressions*.

Figure 8.1 shows the variables ρ, θ, ϕ for the robot arm as a function of time. We also show in Figure 8.2 the controls u_ρ, u_θ, u_ϕ as a function of time. Note that the controls for the robot arm are bang-bang. Also note that the functions ρ, θ, ϕ for the robot arm are continuously differentiable, but since the second derivatives are directly proportional to the controls, the second derivatives are piecewise continuous.

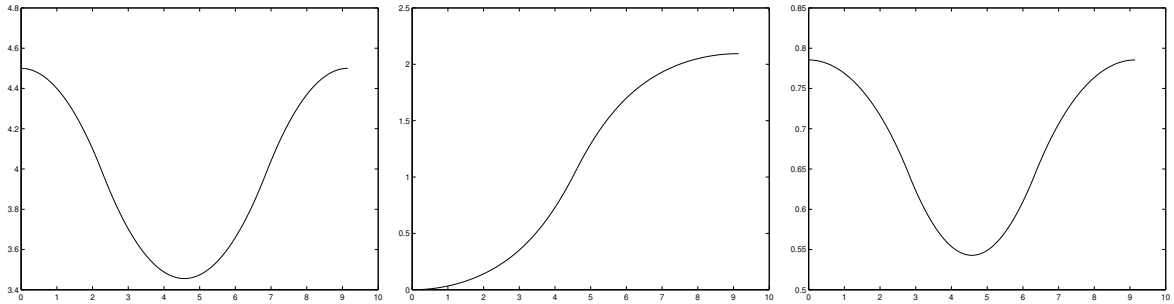

Figure 8.1: Variables ρ, θ, ϕ for the robot arm as a function of time

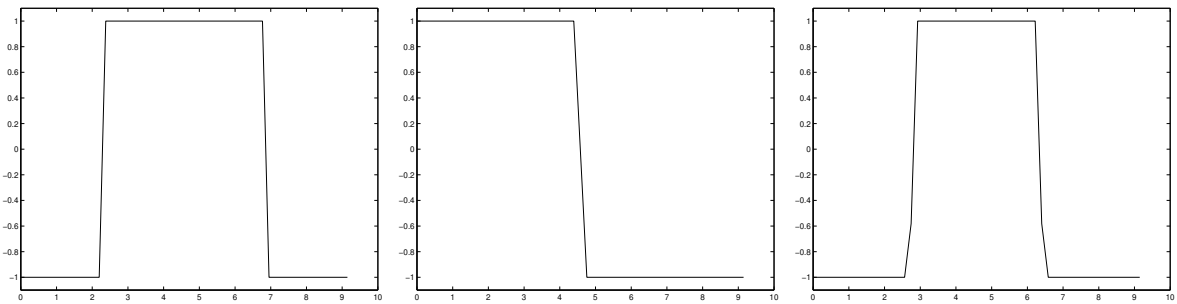

Figure 8.2: Control variables u_ρ, u_θ, u_ϕ for the robot arm as a function of time

9 Particle Steering

Minimize the time taken for a particle, acted upon by a thrust of constant magnitude, to achieve a given altitude and terminal velocity.

Formulation

The equations of motion are

$$\ddot{y}_1 = a\cos(u), \qquad \ddot{y}_2 = a\sin(u), \tag{9.1}$$

where (y_1, y_2) is the position of the particle, u is the control angle with

$$|u(t)| \leq \frac{\pi}{2},$$

and a is the constant magnitude of thrust. The particle is initially at rest so that

$$y_1(0) = y_2(0) = \dot{y}_1(0) = \dot{y}_2(0) = 0.$$

The problem is to minimize the travel time t_f so that the particle achieves a given height $y_2(t_f)$ and terminal velocity $(\dot{y}_1(t_f), \dot{y}_2(t_f))$.

This is a classical (see Bryson and Ho [7, pages 59–62]) problem in dynamic optimization. We use $a = 100$ for the magnitude of thrust and the boundary conditions [4]

$$y_2(t_f) = 5, \qquad \dot{y}_1(t_f) = 45, \qquad \dot{y}_2(t_f) = 0.$$

Discretization is done using a uniform time step and the trapezoidal rule for the integration of the system over n_h intervals. Data for this problem is shown in Table 9.1.

Table 9.1: Particle steering problem data

Variables	$5(n_h + 1) + 1$
Constraints	$4n_h$
Bounds	$n_h + 1$
Linear equality constraints	0
Linear inequality constraints	0
Nonlinear equality constraints	$4n_h$
Nonlinear inequality constraints	0
Nonzeros in $\nabla^2 f(x)$	0
Nonzeros in $c'(x)$	$20n_h$

Performance

Results for the AMPL implementation are given in Table 9.2. The initial values for y_2 and $y_3 = \dot{y}_1$ are chosen as the functions

$$y_1(t) = 5\left(\frac{t}{t_f}\right), \qquad y_3(t) = 45\left(\frac{t}{t_f}\right).$$

Table 9.2: Performance on particle steering problem

Solver	$n_h = 50$	$n_h = 100$	$n_h = 200$	$n_h = 400$
LANCELOT	30.83 s	124.62 s	412.89 s	2997.88 s
f	5.54672e-01	5.54594e-01	5.54588e-01	5.54552e-01†
c violation	2.69440e-06	1.94910e-06	6.12610e-06	8.56120e-06†
iterations	366	416	410	575
LOQO	923.3 s	‡	‡	‡
f	5.54668e-01	‡	‡	‡
c violation	4.1e-10	‡	‡	‡
iterations	20163	‡	‡	‡
MINOS	1.58 s	5.62 s	27.86 s	143.09 s
f	5.54668e-01	5.54595e-01	5.54577e-01	5.54572e-01
c violation	2.5e-13	1.1e-08	2.4e-13	7.9e-10
iterations	278	505	1129	2706
SNOPT	3.25 s	13.43 s	53.81 s	147.37 s
f	5.54668e-01	5.54595e-01	5.54577e-01	5.54573e-01
c violation	5.7e-08	1.9e-09	6.8e-09	5.4e-07
iterations	505	650	1246	2386

† Errors or warnings. ‡ Timed out.

Initial values for y_2, $y_4 = \dot{y}_2$, and u are set to zero. The initial value for the final time is $t_f = 1$. Plots of the height y_2 and control u as a function of the horizontal position y_1 are in Figure 9.1.

Only LANCELOT returns an error here, for $n_h = 400$, of *step got too small*. Even so, it comes near to the optimal solution value.

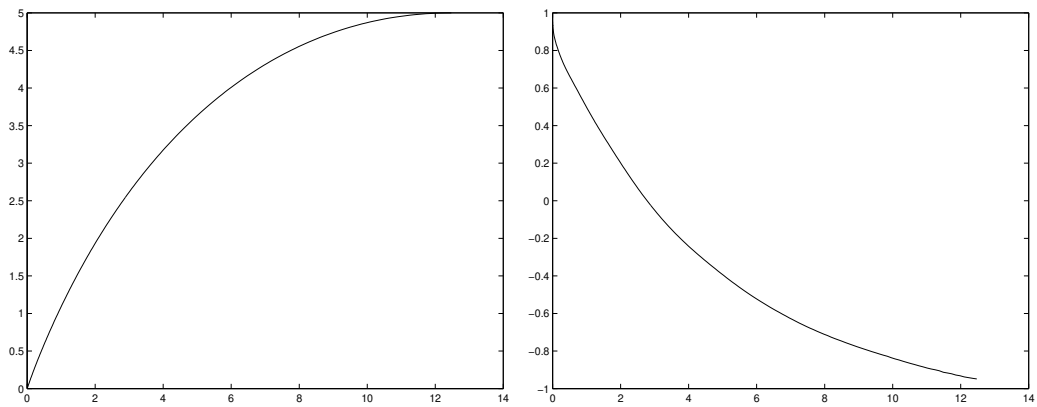

Figure 9.1: Height and control as a function of position for the particle steering problem

10 Goddard Rocket

Maximize the final altitude of a vertically launched rocket, using the thrust as a control and given the initial mass, the fuel mass, and the drag characteristics of the rocket.

Formulation

This is a classical problem in dynamic optimization that is typical of control problems with a singular arc. See Bryson [8, pages 302–394] for background information. The equations of motion for the rocket are

$$h' = v, \qquad v' = \frac{T - D(h,v)}{m} - g(h), \qquad m' = -\frac{T}{c}, \tag{10.1}$$

where h is the altitude from the center of the earth, v is the vertical velocity, T is the rocket thrust, D is the aerodynamic drag, g is the gravitational force, and c is a constant that measures the impulse of the rocket fuel. The thrust must satisfy

$$0 \le T(t) \le T_{\max}.$$

The drag and the gravitational force are defined by

$$D(h,v) = \tfrac{1}{2} D_c v^2 \exp\left(-h_c\left(\frac{h - h(0)}{h(0)}\right)\right), \qquad g(h) = g_0\left(\frac{h(0)}{h}\right)^2,$$

where D_c and h_c are constants, and g_0 is the gravitational force at the earth's surface. The rocket is initially at rest ($v(0) = 0$), and the mass at the end of the flight is a fraction of the initial mass,

$$m(t_f) = m_c m(0),$$

where t_f is the flight time and m_c is a constant. In addition to the bounds on the thrust, there are bounds

$$m(t_f) \le m(t) \le m(0), \qquad h(t) \ge h(0), \qquad v(t) \ge 0,$$

on the mass, altitude, and velocity of the rocket. These bounds are a direct consequence of the equations of motion (10.1).

The equations of motion can be made dimension free by scaling the equations and choosing the model parameters in terms of $h(0)$, $m(0)$, and g_0. We follow [8] and use

$$T_{\max} = 3.5\, g_0 m(0), \qquad D_c = v_c \frac{m(0)}{g_0}, \qquad c = \tfrac{1}{2}(g_0 h(0))^{1/2}.$$

With these choices we can assume, without loss of generality, that $h(0) = m(0) = g_0 = 1$. We also follow [8] and choose

$$h_c = 500, \qquad m_c = 0.6, \qquad v_c = 620.$$

We discretize the equations of motion with the trapezoidal rule, and a uniform mesh with n_h intervals. Data for this problem appears in Table 10.1.

Table 10.1: Goddard rocket problem data

Variables	$4(n_h+1)+1$
Constraints	$3n_h$
Bounds	$3(n_h+1)$
Linear equality constraints	0
Linear inequality constraints	0
Nonlinear equality constraints	$3n_h$
Nonlinear inequality constraints	0
Nonzeros in $\nabla^2 f(x)$	0
Nonzeros in $c'(x)$	$21n_h$

Performance

Results for the AMPL implementation are shown in Table 10.2. For starting points we use $t_f = 1$ and the functions $h = 1$,

$$v(t) = \frac{t}{t_f}\left(1 - \frac{t}{t_f}\right), \qquad m(t) = (m_f - m_0)\left(\frac{t}{t_f}\right) + m_0,$$

evaluated at the grid points. The initial value for the thrust is $T = T_{\max}/2$.

For the rocket problem with $n_h = 200,\ 400$, MINOS makes no progress, declaring it to be an *unbounded (or badly scaled) problem.*

Table 10.2: Performance on Goddard rocket problem

Solver	$n_h = 50$	$n_h = 100$	$n_h = 200$	$n_h = 400$
LANCELOT	‡	‡	‡	‡
f	‡	‡	‡	‡
c violation	‡	‡	‡	‡
iterations	‡	‡	‡	‡
LOQO	3.34 s	3.38 s	4.65 s	12.42 s
f	1.01281e+00	1.01283e+00	1.01283e+00	1.01283e+00
c violation	2.1e-10	4.5e-10	8.2e-10	7.5e-10
iterations	123	64	43	48
MINOS	1.69 s	4.48 s	1.12 s	3.93 s
f	1.01280e+00	1.01278e+00	9.85326e+03†	6.11246e+03†
c violation	4.8e-13	6.1e-16	3.6e+03†	1.1e+03†
iterations	638	378	191	334
SNOPT	3.04 s	9.5 s	31.5 s	64.48 s
f	1.01281e+00	1.01280e+00	1.01281e+00	1.01238e+00
c violation	1.9e-09	4.1e-08	3.5e-09	5.2e-07
iterations	1014	2047	1658	2665

† Errors or warnings. ‡ Timed out.

Figure 10.1 shows the altitude and mass of the rocket as a function of time. Note that altitude increases until a maximum altitude of $h = 1.01$ is reached, while the mass of the rocket steadily decreases until the final mass of $m(t_f) = 0.6$ is reached at $t = 0.073$.

Figure 10.2 shows the velocity and thrust as a function of time. The thrust is bang-singular-bang, with the region of singularity occurring when

$$0 < T(t) < T_{\max}.$$

This figure shows that the optimal flight path involves using maximal thrust until $t = 0.022$, and no thrust for $t \geq 0.073$, at which point the final mass is reached, and the rocket coasts to its maximal altitude. The oscillations that appear at the point of discontinuity in the thrust parameter can be removed by using more grid points.

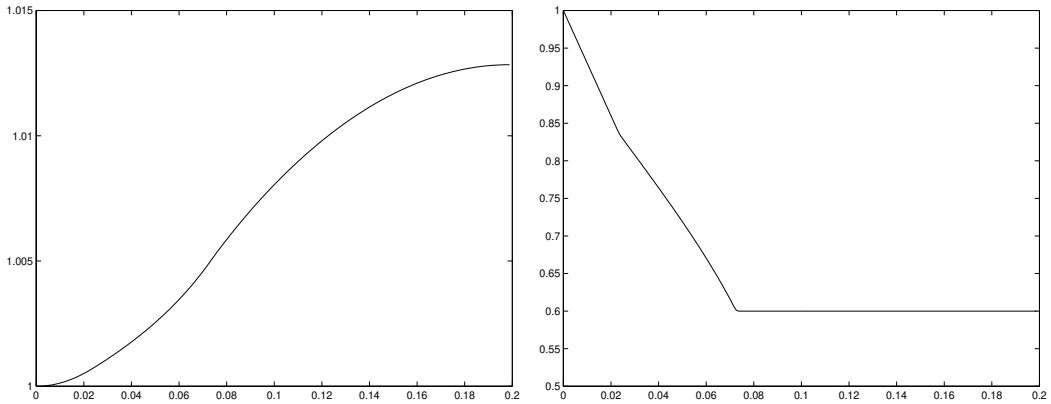

Figure 10.1: Altitude and mass for the Goddard rocket problem

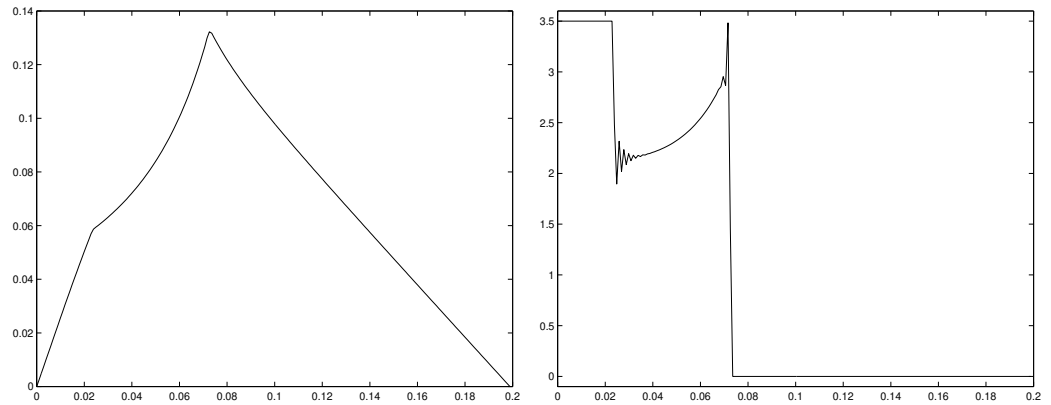

Figure 10.2: Velocity and thrust for the Goddard rocket problem

11 Hang Glider

Maximize the final horizontal position of a hang glider while in the presence of a thermal updraft.

Formulation

The formulation of this problem follows [9]. The equations of motion for the hang glider are

$$x'' = \frac{1}{m}(-L\sin(\eta) - D\cos(\eta)), \qquad y'' = \frac{1}{m}(L\cos(\eta) - D\sin(\eta)) - g, \tag{11.1}$$

where (x, y) is the position of the glider, m is the mass of the glider, g is the gravitational constant, and the function η is defined by

$$\sin(\eta) = \frac{w(x, y')}{v(x, x', y')}, \qquad \cos(\eta) = \frac{x'}{v(x, x', y')},$$

where

$$v(x, x', y') = \sqrt{x'^2 + w(x, y')^2}, \qquad w(x, y') = y' - u(x),$$

$$u(x) = u_c(1 - r(x))\exp(-r(x)), \qquad r(x) = \left(\frac{x}{r_c} - 2.5\right)^2,$$

and constants $u_c = 2.5$ and $r_c = 100$. The updraft function u is positive in a neighborhood of $x = 2.5\, r_c$ but drops to zero exponentially away from $x = 2.5\, r_c$. The functions D and L are defined by

$$D(x, x', y', c_L) = \frac{1}{2}\left(c_0 + c_1 c_L^2\right)\rho S v(x, x', y')^2, \qquad L(x, x', y', c_L) = \frac{1}{2}c_L \rho S v(x, x', y')^2,$$

where S is the wing area, ρ is the air density, c_L is the aerodynamic lift coefficient, and $c_0 + c_1 c_L^2$ is the drag coefficient. For this glider

$$c_0 = 0.034, \quad c_1 = 0.069662, \qquad S = 14, \quad \rho = 1.13.$$

The aerodynamic lift coefficient c_L must satisfy the bounds

$$0 \le c_L(t) \le c_{\max},$$

and we also impose the natural bounds $x \ge 0$ and $x' \ge 0$. In this problem $c_{\max} = 1.4$, $m = 100$, $g = 9.81$, and the boundary conditions are

$$x(0) = 0, \qquad y(0) = 1000, \qquad y(t_f) = 900,$$

$$x'(0) = x'(t_f) = 13.23, \qquad y'(0) = y'(t_f) = -1.288.$$

Discretization is done with a uniform time step and the trapezoidal rule over n_h intervals. Data for this problem is shown in Table 11.1.

Table 11.1: Hang glider problem data

Variables	$5(n_h+1)+1$
Constraints	$4n_h$
Bounds	$3(n_h+1)$
Linear equality constraints	0
Linear inequality constraints	0
Nonlinear equality constraints	$4n_h$
Nonlinear inequality constraints	0
Nonzeros in $\nabla^2 f(x)$	0
Nonzeros in $c'(x)$	$25n_h$

Performance

Results for the AMPL implementation are shown in Table 11.2. For starting points we use $t_f = 1$ and the functions $x' = x'(0)$, $y' = y'(0)$, and

$$x(t) = x(0) + x'(0)\left(\frac{t}{t_f}\right), \qquad y(t) = y(0) + (y(t_f) - y(0))\left(\frac{t}{t_f}\right),$$

evaluated at the grid points. The initial value for the control is $c_L(t) = c_{\max}$.

MINOS fails to produce a solution for any of the problem versions we present it, declaring each an *infeasible problem (or bad starting guess)*.

Table 11.2: Performance on hang glider problem

Solver	$n_h = 50$	$n_h = 100$	$n_h = 200$	$n_h = 400$
LANCELOT	‡	211.76 s	693.74 s	‡
f	‡	1.25461e+03	1.24889e+03	‡
c violation	‡	9.32090e-08	2.86060e-07	‡
iterations	‡	383	539	‡
LOQO	‡	2174.8 s	2601.83 s	‡
f	‡	1.25461e+03	1.24880e+03	‡
c violation	‡	2.1e-11	1.6e-12	‡
iterations	‡	14257	7206	‡
MINOS	28.06 s	95.8 s	206.62 s	732.06 s
f	2.12853e+04†	4.55001e+05†	7.47275e+03†	5.93037e+03†
c violation	3.2e+03†	6.0e+06†	6.4e+02†	6.1e+02†
iterations	8959	16538	14768	23488
SNOPT	11.14 s	44.04 s	240.36 s	1268.67 s
f	1.28239e+03	1.25461e+03	1.24889e+03	1.24797e+03
c violation	1.7e-10	1.8e-10	1.2e-11	5.1e-11
iterations	1764	3001	7906	13286

† Errors or warnings. ‡ Timed out.

Figure 11.1 shows the altitude and control function c_L as a function of time. The glider starts at an altitude of $y(0) = 1000$ and descends until the glider meets the updraft centered at $x = 250$. As a result the glider climbs and then descends to the desired final altitude of $y(t_f) = 900$ at time $t_f = 105$.

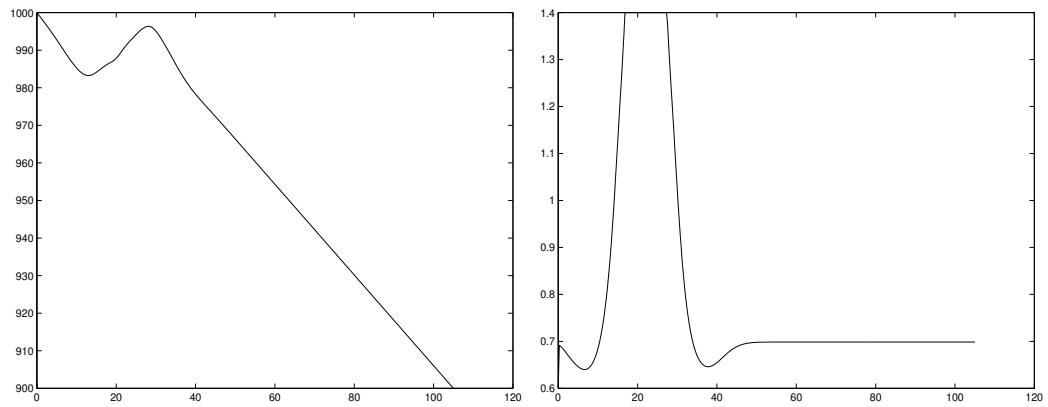

Figure 11.1: Altitude and control c_L for the hang glider problem

Figure 11.2 shows velocities x' and y' as a function of time. Note, in particular, the erratic behavior of the velocities while the control is in the bang-region where $c_L(t) = c_{\max}$.

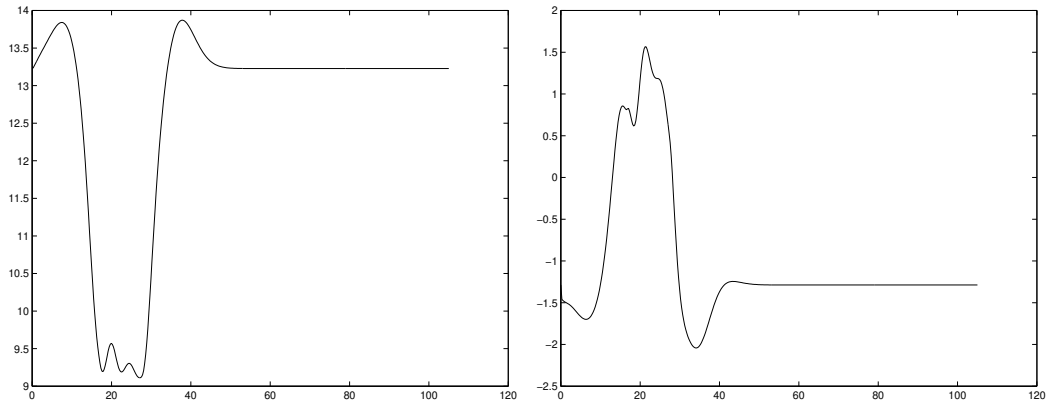

Figure 11.2: Velocities x' and y' for the hang glider problem

12 Catalytic Cracking of Gas Oil

Determine the reaction coefficients for the catalytic cracking of gas oil into gas and other byproducts. The nonlinear model [21] that describes the process is

$$\begin{aligned} y_1' &= -(\theta_1 + \theta_3) y_1^2 \\ y_2' &= \theta_1 y_1^2 - \theta_2 y_2 \end{aligned} \tag{12.1}$$

with coefficients $\theta_i \geq 0$ for $i = 1, \ldots, 3$. Initial conditions for (12.1) are known. The problem is to minimize

$$\sum_{j=1}^{20} \|y(\tau_j; \theta) - z_j\|^2,$$

where z_j are concentration measurements for y at time points $\tau_1, \ldots, \tau_{20}$.

Formulation

Our formulation of the catalytic cracking of gas oil problem as an optimization problem follows [21, 3]. We use a k-stage collocation method, a uniform partition of the interval $[0, \tau_{20}]$ with n_h intervals, and the standard [2, pages 247249] basis representation,

$$v_i + \sum_{j=1}^{k} \frac{(t - t_i)^j}{j!\, h^{j-1}} w_{ij}, \qquad t \in [t_i, t_{i+1}],$$

for the components of the solution (y_1, y_2) of (12.1). The constraints in the optimization problem are the initial conditions in (12.1), the continuity conditions, and the collocation equations. The continuity equations are a set of $2(n_h - 1)$ linear equations. The collocation equations are a set of $2kn_h$ nonlinear equations obtained by requiring that the collocation approximation satisfy (12.1) at the collocation points. Data for this problem appears in Table 12.1.

Table 12.1: Catalytic cracking of gas oil data

Variables	$2(k+1)n_h + 3$
Constraints	$2(k+1)n_h$
Bounds	3
Linear equality constraints	$2n_h$
Linear inequality constraints	0
Nonlinear equality constraints	$2kn_h$
Nonlinear inequality constraints	0
Nonzeros in $\nabla^2 f(x)$	$40k^2$
Nonzeros in $c'(x)$	$3k(k+1)n_h$

Performance

We provide results for the AMPL formulation with $k = 4$ in Table 12.2. The initial values for the θ parameters are $\theta_i = 0.0$. The initial basis parameters are chosen so that the collocation

approximation is piecewise constant and interpolates the data. Data is generated by solving (12.1) numerically using the Tjoa and Biegler [21] values $\theta = (12, 8, 2)$ and applying a relative random perturbation of size 10^{-1}. Figure 12.1 shows the solution and the data.

Table 12.2: Performance on catalytic cracking of gas oil problem

Solver	$n_h = 50$	$n_h = 100$	$n_h = 200$	$n_h = 400$
LANCELOT	918.28 s	3502.88 s	‡	‡
f	5.23633e-03	5.23471e-03	‡	‡
c violation	2.51920e-07	6.72780e-07	‡	‡
iterations	575	993	‡	‡
LOQO	1.37 s	3.36 s	11.6 s	49.62 s
f	5.23664e-03	5.23659e-03	5.23659e-03	5.23659e-03
c violation	2.8e-09	1.8e-09	1.9e-09	1.1e-09
iterations	21	22	31	43
MINOS	5.04 s	14.66 s	49.56 s	161.99 s
f	5.23664e-03	5.23659e-03	5.23659e-03	5.23659e-03
c violation	2.5e-10	9.3e-12	1.3e-08	5.9e-09
iterations	332	550	926	1456
SNOPT	5.25 s	14.41 s	48.56 s	179.71 s
f	5.23664e-03	5.23659e-03	5.23659e-03	5.23659e-03
c violation	2.0e-10	1.4e-08	2.2e-08	4.2e-07
iterations	550	1125	2198	4199

† Errors or warnings. ‡ Timed out.

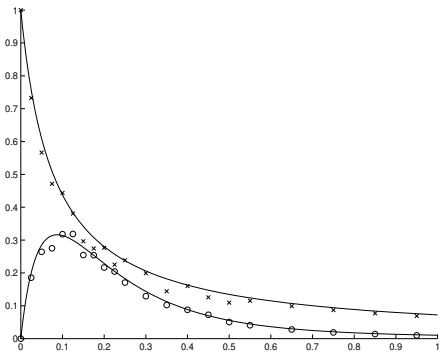

Figure 12.1: Solution and data for the catalytic cracking of gas oil problem

13 Methanol to Hydrocarbons

Determine the reaction coefficients for the conversion of methanol into various hydrocarbons. The nonlinear model [12, 17] that describes the process is

$$\begin{aligned} y_1' &= -\left(2\theta_2 - \frac{\theta_1 y_2}{(\theta_2+\theta_5)y_1 + y_2} + \theta_3 + \theta_4\right) y_1 \\ y_2' &= \frac{\theta_1 y_1(\theta_2 y_1 - y_2)}{(\theta_2+\theta_5)y_1 + y_2} + \theta_3 y_1 \\ y_3' &= \frac{\theta_1 y_1(y_2 + \theta_5 y_1)}{(\theta_2+\theta_5)y_1 + y_2} + \theta_4 y_1 \end{aligned} \tag{13.1}$$

with coefficients $\theta_i \geq 0$ for $i = 1, \ldots, 5$. Initial conditions for (13.1) are known. The problem is to minimize

$$\sum_{j=1}^{16} \|y(\tau_j;\theta) - z_j\|^2,$$

where z_j are concentration measurements for y at time points $\tau_1, \ldots, \tau_{16}$.

Formulation

Our formulation of the methanol-to-hydrocarbons problem as an optimization problem follows [21, 3]. We use a k-stage collocation method, a uniform partition of the interval $[0, \tau_{16}]$ with n_h intervals, and the standard [2, pages 247-249] basis representation,

$$v_i + \sum_{j=1}^{k} \frac{(t-t_i)^j}{j!\, h^{j-1}} w_{ij}, \qquad t \in [t_i, t_{i+1}],$$

for the components of the solution (y_1, y_2, y_3) of (13.1). The constraints in the optimization problem are the initial conditions in (13.1), the continuity conditions, and the collocation equations. The continuity equations are a set of $3(n_h - 1)$ linear equations. The collocation equations are a set of $3kn_h$ nonlinear equations obtained by requiring that the collocation approximation satisfy (13.1) at the collocation points. Data for this problem appears in Table 13.1.

Table 13.1: Methanol-to-hydrocarbons data

Variables	$3(k+1)n_h + 5$
Constraints	$3(k+1)n_h$
Bounds	5
Linear equality constraints	$3n_h$
Linear inequality constraints	0
Nonlinear equality constraints	$3kn_h$
Nonlinear inequality constraints	0
Nonzeros in $\nabla^2 f(x)$	$48k^2$
Nonzeros in $c'(x)$	$7k(k+1)n_h$

Performance

We provide results for the AMPL formulation with $k = 3$ in Table 13.2. The initial values for the θ parameters are $\theta_i = 1.0$. The initial basis parameters are chosen so that the collocation approximation is piecewise constant and interpolates the data. Data is generated by solving (13.1) numerically using $\theta = (2.69, 0.5, 3.02, 0.5, 0.5)$ as given in Maria [17] and applying a relative random perturbation of size 10^{-1}. Figure 13.1 shows the solution and the data.

Table 13.2: Performance on methanol-to-hydrocarbons problem

Solver	$n_h = 50$	$n_h = 100$	$n_h = 200$	$n_h = 400$
LANCELOT	196.62 s	1792.75 s	‡	‡
f	9.02300e-03	9.00563e-03	‡	‡
c violation	4.92130e-06	4.78630e-06	‡	‡
iterations	251	622	‡	‡
LOQO	2.13 s	5.45 s	18.78 s	45.2 s
f	9.02229e-03	9.02229e-03	9.02229e-03	9.02229e-03
c violation	3.5e-07	4.7e-08	1.7e-07	1.9e-08
iterations	19	21	30	26
MINOS	5.05 s	13.49 s	41.83 s	263.67 s
f	9.02228e-03	9.02229e-03	9.02228e-03	9.02228e-03
c violation	9.2e-13	9.8e-13	4.4e-12	3.5e-13
iterations	508	924	1432	2942
SNOPT	12.92 s	32.38 s	131.99 s	512.16 s
f	9.02228e-03	9.02229e-03	9.02228e-03	9.02228e-03
c violation	6.8e-09	9.8e-11	1.6e-09	1.3e-09
iterations	690	1298	2479	4983

† Errors or warnings. ‡ Timed out.

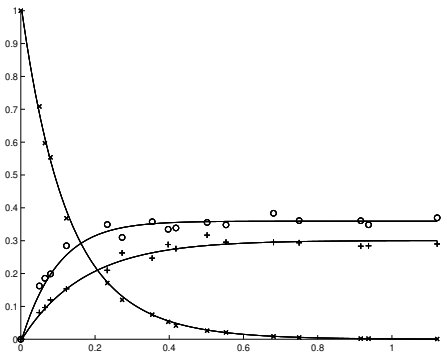

Figure 13.1: Solution and data for the methanol-to-hydrocarbons problem

14 Catalyst Mixing

Determine the optimal mixing policy of two catalysts along the length of a tubular plug flow reactor involving several reactions.

Formulation

The nonlinear model [23] that describes the reactions is

$$\begin{aligned} x_1'(t) &= u(t)(10x_2(t) - x_1(t)) \\ x_2'(t) &= u(t)(x_1(t) - 10x_2(t)) - (1 - u(t))x_2(t). \end{aligned} \tag{14.1}$$

Initial conditions for (14.1) are $x_1(0) = 1$ and $x_2(0) = 0$. The control variable u represents the mixing ratio of the catalysts and must satisfy the bounds

$$0 \leq u(t) \leq 1.$$

The problem is to minimize

$$-1 + x_1(t_f) + x_2(t_f), \tag{14.2}$$

where the final time is fixed at $t_f = 1$.

We discretize the control and state variables along a uniform mesh with n_h intervals and with the standard trapezoidal rule. Data for this problem appears in Table 14.1.

Table 14.1: Catalyst mixing data

Variables	$3(n_h + 1)$
Constraints	$2n_h$
Bounds	$n_h + 1$
Linear equality constraints	0
Linear inequality constraints	0
Nonlinear equality constraints	$2n_h$
Nonlinear inequality constraints	0
Nonzeros in $\nabla^2 f(x)$	0
Nonzeros in $c'(x)$	$12n_h$

Performance

Results for the AMPL implementation are shown in Table 14.2. For starting points we use $u = 0$, $x_1 = 1$, and $x_2 = 0$ evaluated at the grid points.

The catalyst mixing problem is a typical bang-singular-bang problem. The singularity leads to nonunique values of the control in the singular region, and thus it is possible to obtain different values for the control. Figure 14.1 shows the controls obtained by two different solvers.

The results in Table 14.2 show that all the solvers are successful for $n_h \geq 100$ but that the objective function value fluctuates somewhat. This is probably due to the bang-singular-bang nature of the problem. The most common approach to dealing with singular control

Table 14.2: Performance on catalyst mixing problem

Solver	$n_h = 100$	$n_h = 200$	$n_h = 400$	$n_h = 800$
LANCELOT	7.71 s	31.74 s	87.26 s	424.61 s
f	-4.77480e-02	-4.80163e-02	-4.78620e-02	-4.71856e-02
c violation	9.31890e-06	1.03790e-06	2.09770e-06	3.95740e-06
iterations	75	97	100	104
LOQO	0.66 s	1.37 s	3.1 s	8.25 s
f	-4.80694e-02	-4.80591e-02	-4.80565e-02	-4.80559e-02
c violation	7.0e-08	6.4e-08	1.2e-08	1.2e-08
iterations	24	24	24	25
MINOS	2.39 s	5.54 s	5.34 s	17.88 s
f	-4.80605e-02	-4.80302e-02	-4.79881e-02	-4.74787e-02
c violation	2.2e-16	2.2e-16	1.1e-16	1.1e-16
iterations	238	225	105	182
SNOPT	3.99 s	17.32 s	78.72 s	181.24 s
f	-4.80579e-02	-4.80471e-02	-4.80429e-02	-4.80451e-02
c violation	1.8e-08	1.8e-07	3.5e-08	2.0e-05
iterations	369	712	1368	2539

† Errors or warnings. ‡ Timed out.

problems is to add a penalty to the objective function that leads to a smooth control, for example,

$$\alpha \int_0^1 u'(t)^2 \, dt$$

for some positive value of α. Values of $\alpha \geq 1$ seems to work well for this problem, but an appropriate value is difficult to find.

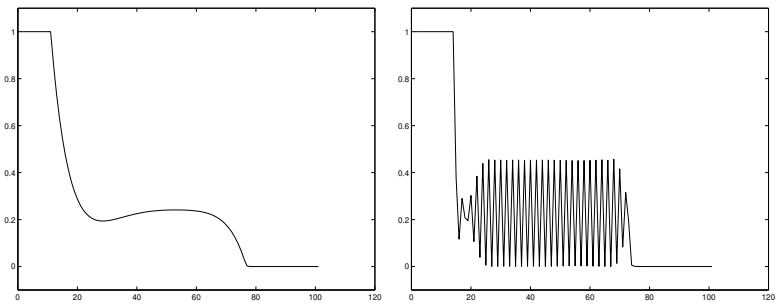

Figure 14.1: Controls obtained by two different solvers for the catalyst mixing problem

15 Elastic-Plastic Torsion

Determine the stress potential in an infinitely long cylinder when torsion is applied.

Formulation

The elastic-plastic torsion problem [15, pages 41–46] can be formulated in terms of the cross-section $\mathcal{D}$ of the cylinder, and the torsion angle c per unit length. The stress potential u minimizes the quadratic $q : K \mapsto \mathbb{R}$,

$$q(v) = \int_{\mathcal{D}} \left\{ \frac{1}{2} \|\nabla v(x)\|^2 - c\, v(x) \right\} dx,$$

over the convex set K, where

$$K = \{v \in H_0^1(\mathcal{D}) : |v| \leq dist(x, \partial\mathcal{D}),\ x \in \mathcal{D}\},$$

$dist(x, \partial\mathcal{D})$ is the distance from x to the boundary of $\mathcal{D}$, and $H_0^1(\mathcal{D})$ is the space of functions with gradients in $L^2(\mathcal{D})$ that vanish on the boundary of $\mathcal{D}$.

A finite element approximation to the elastic-plastic torsion problem is obtained by triangulating $\mathcal{D}$ and minimizing q over the space of piecewise linear functions with values $v_{i,j}$ at the vertices of the triangulation. We follow [15, 3] by choosing $\mathcal{D} = [0,1] \times [0,1]$, and using a triangulation with, respectively, n_x and n_y internal grid points in the coordinate directions. Data for this problem appears in Table 15.1.

Table 15.1: Elastic-plastic torsion problem data

Variables	$n_x n_y$
Constraints	0
Bounds	$n_x n_y$
Linear equality constraints	0
Linear inequality constraints	0
Nonlinear equality constraints	0
Nonlinear inequality constraints	0
Nonzeros in $\nabla^2 f(x)$	$5n_x n_y - 2(n_x + n_y)$
Nonzeros in $c'(x)$	0

Performance

We provide results for the AMPL formulation with $c = 5$ in Table 15.2. For these results we fix $n_x = 50$ and vary n_y. The starting guess is the function $dist(x, \partial\mathcal{D})$ evaluated at the grid nodes. Figure 15.1 shows the potential in the torsion problem with $c = 5$. The number of active constraints in this problem increases with c. Also

$$\lim_{c \to \infty} v_c(x) = dist(x, \partial\mathcal{D}),$$

where v_c is the potential as a function of c.

Table 15.2: Performance on elastic-plastic torsion problem

Solver	$n_y = 25$	$n_y = 50$	$n_y = 75$	$n_y = 100$
LANCELOT	3.01 s	7.1 s	11.85 s	17.19 s
f	-4.17510e-01	-4.18087e-01	-4.18199e-01	-4.18239e-01
c violation	0.00000e+00	0.00000e+00	0.00000e+00	0.00000e+00
iterations	14	18	19	21
LOQO	2.99 s	6.94 s	11.55 s	15.86 s
f	-4.17510e-01	-4.18087e-01	-4.18199e-01	-4.18239e-01
c violation	1.9e-15	1.7e-14	3.3e-15	3.7e-15
iterations	19	19	21	21
MINOS	108.31 s	830.16 s	2758.52 s	‡
f	-4.17510e-01	-4.18087e-01	-4.18199e-01	‡
c violation	0.0e+00	0.0e+00	0.0e+00	‡
iterations	910	1775	2656	‡
SNOPT	125.58 s	1207.62 s	‡	‡
f	-4.17510e-01	-4.18087e-01	‡	‡
c violation	0.0e+00	0.0e+00	‡	‡
iterations	1137	2446	‡	‡

† Errors or warnings. ‡ Timed out.

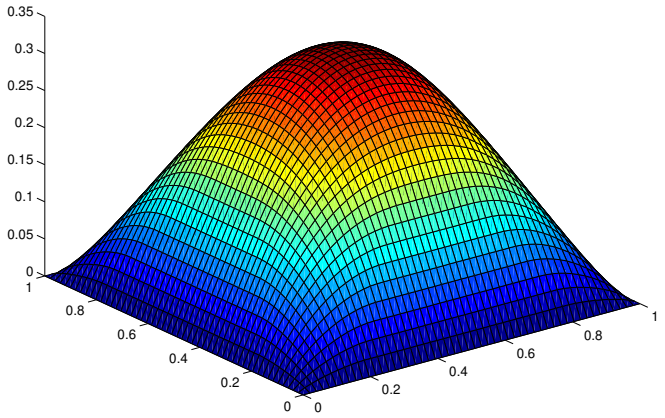

Figure 15.1: Elastic plastic torsion problem with $c = 5$

16 Journal Bearing

Given the eccentricity ϵ of the journal bearing, find the pressure distribution in the lubricant separating the shaft from the bearing.

Formulation

The journal bearing problem [10] requires determining the pressure between two circular cylinders of length L and radii R and $R + c$. The separation between the cylinders is εc, where ε is the eccentricity. The pressure v minimizes the quadratic $q : K \mapsto \mathbb{R}$,

$$q(v) = \int_{\mathcal{D}} \left\{ \frac{1}{2} w_q(x) \|\nabla v(x)\|^2 - w_l(x) v(x) \right\} dx,$$

over the convex set K, where $\mathcal{D} = (0, 2\pi) \times (0, 2b)$,

$$K = \{v \in H_0^1(\mathcal{D}) : v \geq 0\},$$

$H_0^1(\mathcal{D})$ is the space of functions with gradients in $L^2(\mathcal{D})$ that vanish on the boundary of $\mathcal{D}$, and the functions $w_q : \mathcal{D} \mapsto \mathbb{R}$ and $w_l : \mathcal{D} \mapsto \mathbb{R}$ are defined by

$$w_q(\xi_1, \xi_2) = (1 + \varepsilon \cos \xi_1)^3, \qquad w_l(\xi_1, \xi_2) = \varepsilon \sin \xi_1,$$

with $\varepsilon \in (0, 1)$ the eccentricity of the bearing.

A finite element approximation to the journal bearing problem is obtained by triangulating $\mathcal{D}$ and minimizing q over the space of piecewise linear functions with values $v_{i,j}$ at the vertices of the triangulation. We follow [3] by using a triangulation with, respectively, n_x and n_y internal grid points in the coordinate directions. Data for this problem appears in Table 16.1.

Table 16.1: Journal bearing problem data

Variables	$n_x n_y$
Constraints	0
Bounds	$n_x n_y$
Linear equality constraints	0
Linear inequality constraints	0
Nonlinear equality constraints	0
Nonlinear inequality constraints	0
Nonzeros in $\nabla^2 f(x)$	$5n_x n_y - 2(n_x + n_y)$
Nonzeros in $c'(x)$	0

Performance

We provide results with the AMPL formulation in Table 16.2 with $b = 10$ and $\epsilon = 0.1$. For these results we fix $n_x = 50$ and vary n_y. The starting guess is the function $\max\{\sin(x), 0\}$ evaluated at the grid nodes. Figure 16.1 shows the pressure distribution for the journal bearing problem.

Table 16.2: Performance on pressure in journal bearing problem

Solver	$n_y = 25$	$n_y = 50$	$n_y = 75$	$n_y = 100$
LANCELOT	3.02 s	7.19 s	11.77 s	17.89 s
f	-1.54015e-01	-1.54824e-01	-1.54984e-01	-1.55042e-01
c violation	0.00000e+00	0.00000e+00	0.00000e+00	0.00000e+00
iterations	12	11	10	10
LOQO	3.36 s	5.71 s	9.56 s	13.33 s
f	-1.54015e-01	-1.54824e-01	-1.54984e-01	-1.55042e-01
c violation	2.2e-16	3.1e-16	3.7e-16	4.2e-16
iterations	26	19	20	21
MINOS	173.65 s	964.59 s	2850.41 s	‡
f	-1.54015e-01	-1.54824e-01	-1.54984e-01	‡
c violation	0.0e+00	0.0e+00	0.0e+00	‡
iterations	1340	2258	2988	‡
SNOPT	722.68 s	‡	‡	‡
f	-1.54015e-01	‡	‡	‡
c violation	0.0e+00	‡	‡	‡
iterations	3274	‡	‡	‡

† Errors or warnings. ‡ Timed out.

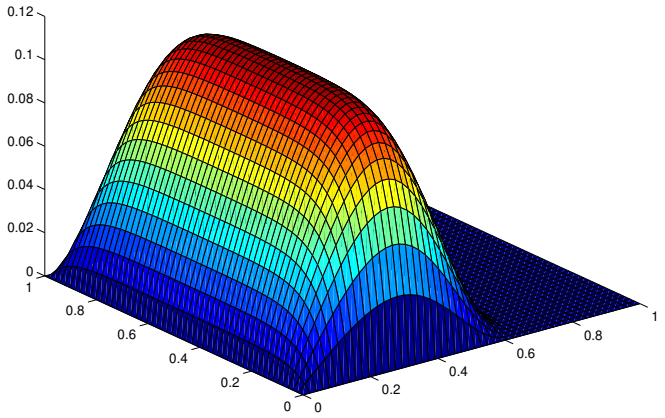

Figure 16.1: Journal bearing problem with $\epsilon = 0.1$

17 Minimal Surface with Obstacle

Find the surface with minimal area, given boundary conditions, and above an obstacle.

Formulation

Plateau's problem is to determine the surface of minimal area with a given closed curve in $\mathbb{R}^3$ as boundary. We assume that the surface can be represented in nonparametric form $v : \mathbb{R}^2 \mapsto \mathbb{R}$, and we add the requirement that $v \geq v_L$ for some obstacle v_L. The solution of this obstacle problem [13] minimizes the function $f : K \mapsto \mathbb{R}$,

$$f(v) = \int_{\mathcal{D}} \left(1 + \|\nabla v(x)\|^2\right)^{1/2} \, dx,$$

over the convex set K, where

$$K = \left\{ v \in H^1(\mathcal{D}) : v(x) = v_D(x) \text{ for } x \in \partial\mathcal{D}, \quad v(x) \geq v_L(x) \text{ for } x \in \mathcal{D} \right\},$$

$H^1(\mathcal{D})$ is the space of functions with gradients in $L^2(\mathcal{D})$, the function $v_D : \partial\mathcal{D} \mapsto \mathbb{R}$ defines the boundary data, and $v_L : \mathcal{D} \mapsto \mathbb{R}$ is the obstacle. We assume that $v_L \leq v_D$ on the boundary $\partial\mathcal{D}$.

A finite element approximation to the minimal surface problem is obtained by triangulating $\mathcal{D}$ and minimizing f over the space of piecewise linear functions with values $v_{i,j}$ at the vertices of the triangulation. We set $\mathcal{D} = [0,1] \times [0,1]$ and use a triangulation with, respectively, n_x and n_y internal grid points in the coordinate directions. Data for this problem appears in Table 16.1.

Table 17.1: Minimal surface problem data

Variables	$n_x n_y$
Constraints	0
Bounds	$n_x n_y$
Linear equality constraints	0
Linear inequality constraints	0
Nonlinear equality constraints	0
Nonlinear inequality constraints	0
Nonzeros in $\nabla^2 f(x)$	$5n_x n_y - 2(n_x + n_y)$
Nonzeros in $c'(x)$	0

Performance

We provide results for the AMPL formulation in Table 17.2. For these results we fix $n_x = 50$ and vary n_y. The starting guess is the function $1 - (2x - 1)^2$ evaluated at the grid nodes. We used boundary data

$$v_D(x, y) = \begin{cases} 1 - (2x - 1)^2, & y = 0, 1 \\ 0, & \text{otherwise,} \end{cases}$$

and the obstacle

$$v_L(x,y) = \begin{cases} 1 & \text{if } |x - \frac{1}{2}| \leq \frac{1}{4},\ |y - \frac{1}{2}| \leq \frac{1}{4} \\ 0, & \text{otherwise.} \end{cases}$$

Figure 17.1 shows the minimal surface for this data.

Table 17.2: Performance on minimal surface area with obstacle problem

Solver	$n_y = 25$	$n_y = 50$	$n_y = 75$	$n_y = 100$
LANCELOT	2.77 s	5.9 s	10.34 s	16.33 s
f	2.51948e+00	2.51488e+00	2.50568e+00	2.50694e+00
c violation	0.00000e+00	0.00000e+00	0.00000e+00	0.00000e+00
iterations	8	9	10	13
LOQO	2.98 s	9.76 s	23.32 s	‡
f	2.51948e+00	2.51488e+00	2.50568e+00	‡
c violation	2.4e-15	3.8e-15	3.4e-15	‡
iterations	20	28	46	‡
MINOS	103.76 s	984.81 s	‡	‡
f	2.51948e+00	2.51488e+00	‡	‡
c violation	0.0e+00	0.0e+00	‡	‡
iterations	901	1970	‡	‡
SNOPT	137.88 s	‡	‡	‡
f	2.51948e+00	‡	‡	‡
c violation	0.0e+00	‡	‡	‡
iterations	1001	‡	‡	‡

† Errors or warnings. ‡ Timed out.

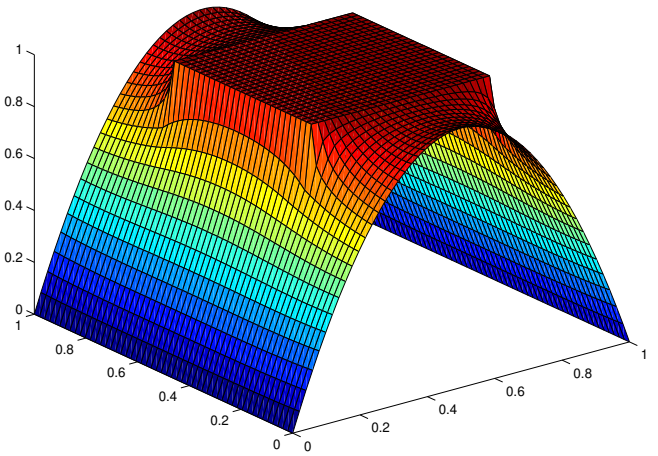

Figure 17.1: Minimal surface problem with a plate obstacle

Acknowledgments

Version 1.0 of the COPS problems was developed by Alexander Bondarenko, David Bortz, Liz Dolan, and Michael Merritt. Their contributions were essential because, in many cases, version 2.0 of the problems are closely related to the original version.

Bob Vanderbei contributed with several interesting and spirited discussions on problem formulation, while Bob Fourer and David Gay generously shared their AMPL expertise with us. Finally, we thank Hans Mittelmann for paving the way for COPS with his benchmarking work.

References

[1] M. Anitescu and R. Serban, *A sparse superlinearly convergent SQP with applications to two-dimensional shape optimization*, Preprint ANL/MCS-P706-0198, Argonne National Laboratory, Argonne, Illinois, 1998.

[2] U. M. Ascher, R. M. M. Mattheij, and R. D. Russell, *Numerical solution of boundary value problems for ordinary differential equations*, SIAM, 1995.

[3] B. M. Averick, R. G. Carter, J. J. Moré, and G.-L. Xue, *The MINPACK-2 test problem collection*, Preprint MCS-P153-0694, Mathematics and Computer Science Division, Argonne National Laboratory, Argonne, Illinois, 1992.

[4] J. Betts, S. Eldersveld, and W. Huffman, *Sparse nonlinear programming test problems (Release 1.0)*, Technical report BCSTECH-93-047, Boeing Computer Services, Seattle, Washington, 1993.

[5] A. S. Bondarenko, D. M. Bortz, and J. J. Moré, *COPS: Large-scale nonlinearly constrained optimization problems*, Technical Memorandum ANL/MCS-TM-237, Argonne National Laboratory, Argonne, Illinois, 1998 (Revised October 1999).

[6] G. E. P. Box, W. G. Hunter, J. F. MacGregor, and J. Erjavec, *Some problems associated with the analysis of multiresponse data*, Technometrics, 15 (1973), pp. 33–51.

[7] A. Bryson and Y. Ho, *Applied Optimal Control: Optimization, Estimation, and Control*, John Wiley & Sons, 1975.

[8] A. E. Bryson, *Dynamic Optimization*, Addison-Wesley, 1999.

[9] R. Bulirsch, E. Nerz, H. J. Pesch, and O. von Stryk, *Combining direct and indirect methods in nonlinear optimal control: Range maximization of a hang glider*, in Optimal Control, R. Bulirsch, A. Miele, J. Stoer, and K. H. Well, eds., Birkhäuser Verlag, 1993, pp. 273–288.

[10] G. Capriz and G. Cimatti, *Free boundary problems in the theory of hydrodynamic lubrication: A survey*, in Free Boundary Problems: Theory and Applications, A. Fasano and M. Primicerio, eds., no. 79 in Research Notes in Mathematics, Pitman, 1983, pp. 613–635.

[11] L. Cesari, *Optimization - Theory and Applications*, Springer Verlag, 1983.

[12] C. A. Floudas, P. M. Pardalos, C. S. Adjiman, W. R. Esposito, Z. H. Gumus, S. T. Harding, J. L. Klepeis, C. A. Meyer, and C. A. Schweiger, *Handbook of Test Problems for Local and Global Optimization*, Kluwer Academic Publishers, 1999.

[13] A. Friedman, *Free boundary problems in science and technology*, Notices Amer. Math. Soc., 47 (2000), pp. 854–861.

[14] D. Gay, *AMPL models*. See `http://www.netlib.org/ampl/models/`.

[15] R. Glowinski, *Numerical Methods for Nonlinear Variational Problems*, Springer-Verlag, 1984.

[16] R. L. Graham, *The largest small hexagon*, J. Combin. Th., 18 (1975), pp. 165–170.

[17] G. Maria, *An adaptive strategy for solving kinetic model concomitant estimation - reduction problems*, Can. J. Chem. Eng., 67 (1989), p. 825.

[18] J. R. Morris, D. M. Deaven, and K. M. Ho, *Genetic algorithm energy minimization for point charges on a sphere*, Phys. Rev. B, 53 (1996), pp. R1740–R1743.

[19] B. J. Rothschild, A. F. Sharov, A. J. Kearsley, and A. S. Bondarenko, *Estimating growth and mortality in stage-structured populations*, Journal of Plankton Research, 19 (1997), pp. 1913–1928.

[20] E. B. Saff and A. Kuijlaars, *Distributing many points on the sphere*, Math. Intelligencer, 19 (1997), pp. 5–11.

[21] I.-B. Tjoa and L. T. Biegler, *Simultaneous solution and optimization strategies for parameter estimation of differential-algebraic equations systems*, Ind. Eng. Chem. Res., 30 (1991), pp. 376–385.

[22] R. Vanderbei, *Nonlinear optimization models*. See `http://www.sor.princeton.edu/~rvdb/ampl/nlmodels/`.

[23] O. von Stryk, *User's guide for DIRCOL (Version 2.1): A direct collocation method for the numerical solution of optimal control problems*, technical report, Technische Universität München, 1999.